Dual-Band Single-Layer Slot Array Antenna Fed by K/Ka-Band Dual-Mode Resonators in Gap Waveguide Technology

Miguel Ferrando-Rocher, *Member, IEEE,* Jose I. Herranz-Herruzo, *Member, IEEE,*
Alejandro Valero-Nogueira, *Senior Member, IEEE,* Mariano Baquero-Escudero *Senior Member, IEEE*

***Abstract*—This paper presents a 4×4 single-layer dual-band array antenna operating in K and Ka-band using Gap Waveguide technology (GW). Radiating elements consist of I-shaped slots located on the top plate of the antenna and backed by a novel coaxial cavity with dual-frequency operation. The antenna presents two ports, one for each band, and radiates a directive far field pattern with linear polarization. A single-layer wideband corporate-feed network is used to excite the cavities. In addition, a diplexer is integrated as part of the network to separate both working bands. Experimental results show impedance and radiation pattern bandwidths larger than 2 GHz in both bands.**

***Index Terms*—Array, Dual-Band Antenna, Gap Waveguide, Ka-Band, K-Band, SATCOM, Shared-Aperture.**

I. Introduction

SATELLITE communication systems deliver many essential services from hand-held satellite phones and remote site fixed installations, to vessel, vehicular and airborne mobile terminals, offering different performance options to suit the ever-increasing demand of users [1]. In the bidirectional satellite communication systems, downlink and uplink operate in different frequency bands, which are typically centered in 20 and 30 GHz, respectively.

Antennas operating simultaneously on these two bands and with compact size, lightweight, and low cost are particularly desired. In this context, shared-aperture approaches enable to save space and cost on antenna platform, being a demanding target sought by researchers and industry [2]-[6]. Particularly challenging has been the development of low-profile dual-band arrays for K/Ka-band satellite communications due to the large separation of receive and transmit bands.

Over the last decade, countless types of dual-band antennas, either linearly or circularly polarized, have been reported, typically using microstrip technology [7]-[9]. However, most of these contributions present narrow impedance bandwidth or limited antenna efficiency. Specifications for satellite communication antennas often require high directivity and high efficiency with at least 2 GHz of frequency bandwidth in each band.

A promising all-metal approach in that regard was presented in [10], consisting of a a dual-band antenna array in Gap Waveguide (GW) technology. In this antenna, shared circular apertures excited by stacked cylindrical cavities are used as radiating elements. Although contact between layers is not critical thanks to the inherent characteristics of GW technology [11], stacking layers increases the cost, height, weight and volume of the antenna. Besides that, one inherent limitation in such dual-band design is the electrical array spacing, which must be small enough to avoid grating lobes at the higher frequency band. In addition, the large radiator size required to operate on the lower band constrains the space available to host the feeding network.

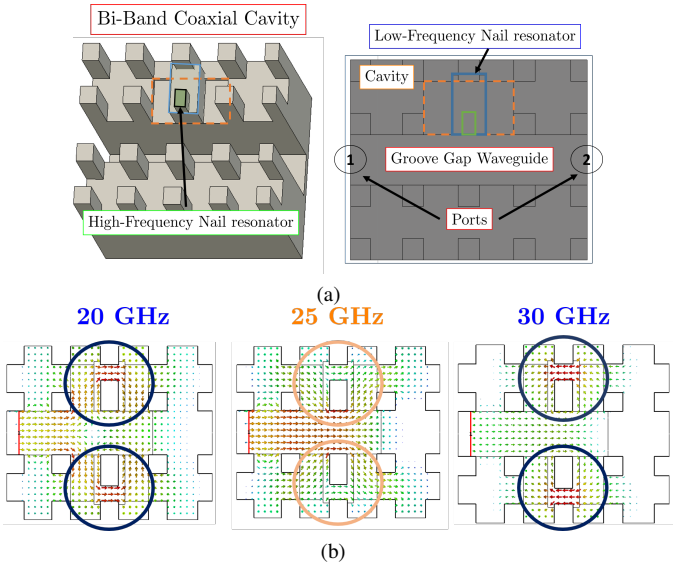

Fig. 1: (a) 3D layout of the unit cell where the coaxial cavity is highlighted. (b) Magnetic field at 20 GHz, 25 GHz and 30 GHz in the cavity.

In this work we propose a dual-band coaxial cavity resonating at two frequencies to excite a radiating I-shaped slot. These cavities are fed by a wideband corporate network sharing the same layer as the radiating elements. The antenna has two inputs, one for transmission and one for reception, which include filters that conform a diplexer at 20 and 30 GHz.

Embedding the diplexer in a single-layer antenna is key to reduce the total size and cost of the system. There exist few examples of diplexers hosted in single-layer full-metal antennas in the millimeter-wave band. For example, diplexers using gap waveguide technology are presented in [12] and [13]. There,

This work has been supported by the Spanish Ministry ofScience and Innovation under the project PID2019-107688RB-C22.

M. Ferrando-Rocher, J. I. Herranz-Herruzo, A. Valero-Nogueira, and M. Baquero-Escudero are with Instituto de Telecomunicaciones y Aplicaciones Multimedia (ITEAM) of the Universitat Politècnica de València, c/ Cami de Vera s/n, 46022 Valencia, Spain (e-mail: miferroc@iteam.upv.es)

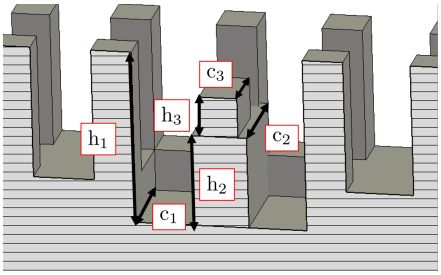

Parameter	Value
h_1	3.9 mm
h_2	2.1 mm
h_3	0.9 mm
c_1	2.2 mm
c_2	2.4 mm
c_3	0.9 mm

Fig. 2: Bi-band coaxial cavity dimensions.

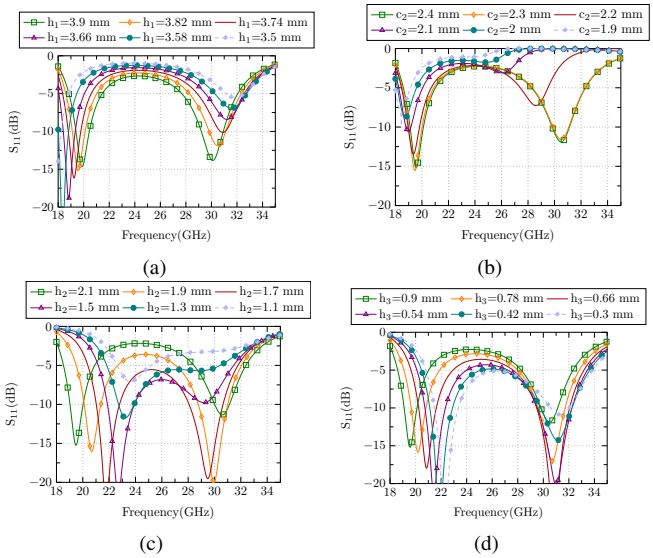

Fig. 3: Parametric study of the key dimensions of the dual-mode resonator: (a) h_1, (b) c_2, (c) h_2 and (d) h_3.

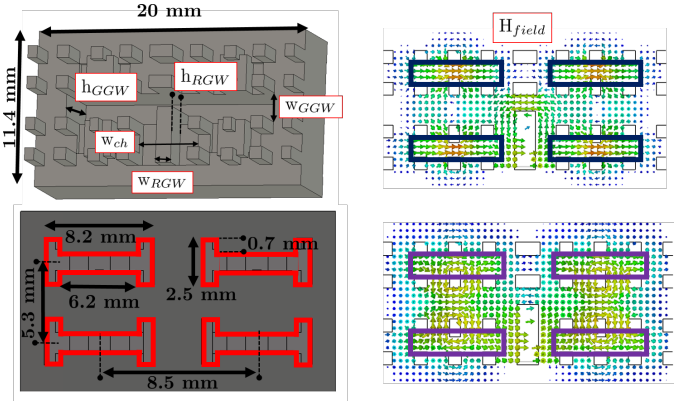

Fig. 4: Layout of the 2×2 array with and without cover (on the left) and magnetic field at each frequency (on the right).

the working bands are much closer together and the diplexers are integrated in dedicated layers in multilevel antennas.

We show a fabricated full aluminum single-layer dual-band shared-aperture array antenna with high efficiency (above 80% in both bands), and wide impedance bandwidth (≥ 2 GHz in both bands). The proposed array architecture is suitable for millimeter-wave dual-band applications. The array architecture allows the antenna size to be easily extended to achieve higher gains if needed.

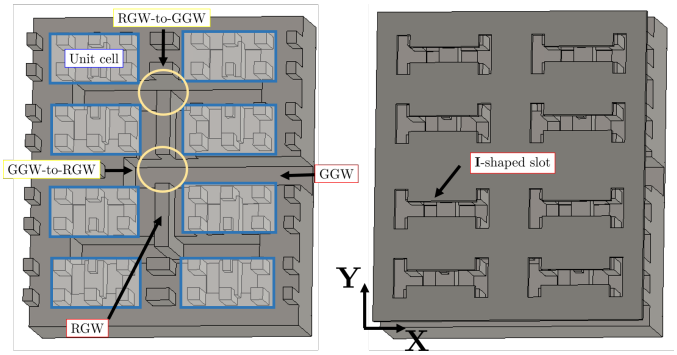

Fig. 5: Layout of the 4×2 antenna indicating the feeding network and the basic cells (on the left) and the array with the lid (on the right).

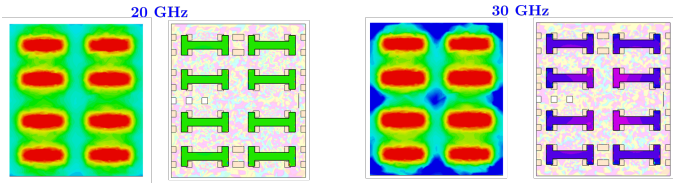

Fig. 6: Module and phase of the aperture E-field for each frequency.

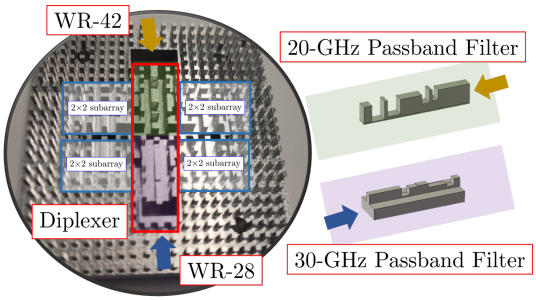

Fig. 7: Diplexer integrated in the antenna. Relevant blocks of the full prototype and input ports are highlighted.

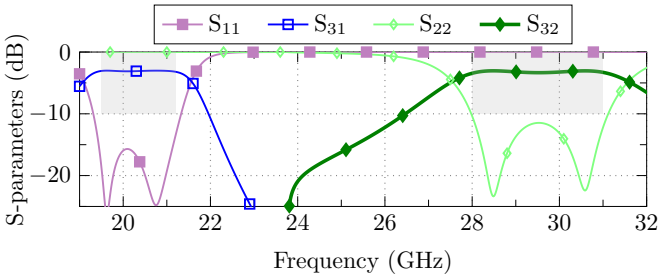

Fig. 8: Simulated performance of the power-divider diplexer.

II. Single-Layer Dual-Band Cavity-Backed Antenna

The unit cell of the array is directly inspired by the coaxial cavities used in previous works [14]-[15]. However, those K-band and V-band arrays, respectively, were single-band antennas. The challenge here has been to modify the coaxial cavity to resonate at two very separate working bands. Not only that, a second challenge has been to design a network compact

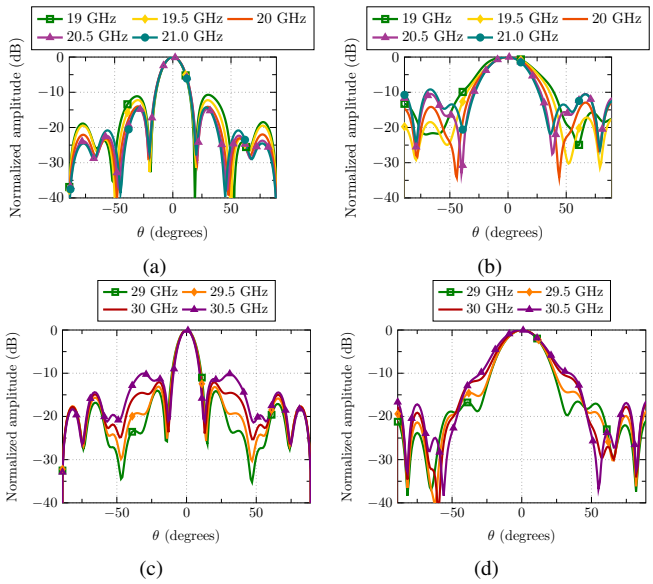

Fig. 9: Normalized simulated copolar patterns at several frequencies using the 4×4 antenna array: K-band port (a) E-plane and (b) H-plane; Ka-band port (c) E-plane and (d) H-plane.

enough to place the slots as close together as physically possible to avoid grating lobes.

The cell presented in Fig. 1 is a coaxial resonator with two operating bands backing a slot. As [14] demonstrated, when a nail is slightly shortened, a coaxial cavity can be created and it resonates at a given frequency when placed close to a field source. The idea here is to stack two nails of different widths and heights, obtaining a sort of a pie shape. In this way, the lower nail acts as the coaxial resonator for the lower band and the upper nail acts as the coaxial resonator in the higher band. Fig. 1b shows how the field is trapped in a similar way at both frequencies. Interestingly, in the frequencies between both bands the field is not coupled with the same intensity, as observed at 25 GHz. All relevant dual-mode resonator dimensions and their values are presented in Fig. 2. In addition, a parametric study is detailed in Fig. 3. The study reveals how the dimension c_2 is key to adjust the upper band resonance and how h_2 and h_3 serve to tune the lower frequency to the resonance of interest. The parameter h_1, which is the total height of the cavity, affects both resonances.

Then, the cell presented in Fig. 1a is progressively replicated to achieve larger arrays. Firstly a 2×2-cell array is presented (Fig. 4), and then the 4×2-cell array is shown in Fig. 5. It should be noted that this dual-band antenna must be fed by a wide-bandwidth corporate-feed network covering both bands, from 19 to 32 GHz. Here a network combining Ridge Gap Waveguides (RGW) and Groove Gap waveguides (GGW) is used. This network has demonstrated to be very useful for single-layer 2D gap waveguide arrays since it was conceived in [16]. In addition, a diplexer is needed to feed the whole system. A diplexer will be located in the central part of the 4×4 antenna and will be described in next section.

Below, these cells and the diplexer are described in more detail with the help of their accompanying figures, Figs. 4 to 6, respectively, to provide a comprehensive description of the structure.

TABLE I: Measured antenna parameters at K-band.

Frequency (GHz)	19.0	19.5	20.0	20.5	21.0
Directivity (dBi)	16.0	16.8	17.3	17.5	17.8
Gain (dBi)	14.37	16.01	16.61	16.72	17.07
Antenna Efficiency (%)	68.54	83.34	85.43	83.68	84.66

TABLE II: Measured antenna parameters at Ka-band.

Frequency (GHz)	29.0	29.5	30.0	30.5	31.0
Directivity (dBi)	19.77	19.39	19.21	18.70	17.85
Gain (dBi)	18.72	18.50	18.46	18.17	16.81
Antenna Efficiency (%)	78.70	81.63	84.30	88.62	78.83

1) 2×2 Array: On the left side of Fig. 4, four cells fed corporately by a RGW-GGW combined network are shown. The dimensions of the cell are indicated as well as the most relevant parameters involved in the feeding network. On the right side of the figure, the magnetic field is shown at 20 GHz (upper image) and 30 GHz (lower image). The area where the magnetic field is intense and where the slots will be located is highlighted. Due to the required compactness of the cell the slots are I-shaped in such a way that they can be resonant at the lower band too. Rectangular slots would have caused a portion of them to be directly over the center feeding waveguide, thus spoiling the array performance. Using a wider separation of the cells would have been another possible solution, but at the expense of increasing the grating lobes in the radiation patterns at the higher band. The I-shaped slots do not increase the crosspolar component values significantly as will be demonstrated experimentally in next section.

2) 4×2 Array: In Fig. 5, the 4×2 array is shown. Antenna input is fed by a GGW. Two of these 4×2 blocks will make up the complete fabricated antenna (4×4). The input GGW, indicated with an arrow coming from the right, will be connected to the K-Ka diplexer. Fig. 6 shows that all the slots are excited with the same amplitude and phase in each band.

3) Diplexer at K/Ka-band: The K-Ka band diplexer is used to connect two of those 4×2 arrays previously described (Fig. 7). The diplexer has been designed with FEST3D tool integrated into CST Studio [17]. The simulated result of both filters is displayed in Fig. 8. The two working bands and the isolation between them are clearly observed. Then, the diplexer is integrated into the antenna. It should be noted that the S-parameters of the 4×2 array have been taken into account in the optimization process of the diplexer, so a good matching of the whole system is expected.

III. 4×4 Array Experimental Demonstrator

Finally, all parts involved are put together to form the 4×4 array. Fig. 9 presents the simulated radiation patterns. E and H planes at different frequencies of both bands are shown. Interesting conclusions are drawn from these radiation patterns. On the one hand, the E-plane in both cases corresponds to a pattern with some stability in both K and Ka bands. Notice how sidelobes grow progressively as frequency increases in the Ka-band, which is expected given the slot spacing. On the other hand, in the YZ-plane (H-plane), the pattern can be

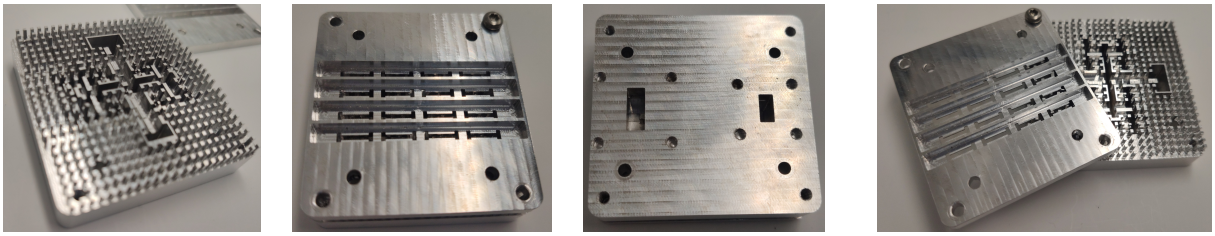

(a) (b) (c) (d)

Fig. 10: Manufactured prototype: (a) Layer integrating the diplexer, the corporate-feed network and resonators; (b) radiating layer; (c) back view of the antenna with the two input ports WR-42 and WR-28 and (d) antenna with the cover slipped

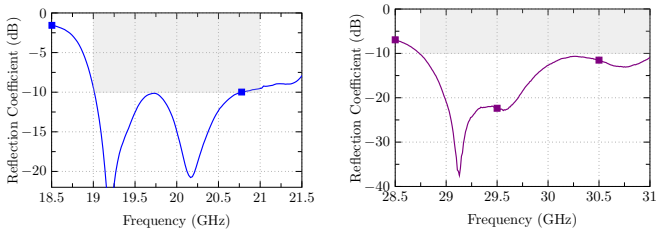

(a) (b)

Fig. 11: Measured reflection coefficient in the K and K band.

affected by the antenna asymmetry, since on one side is placed the 20 GHz filter and on the other side the 30 GHz filter. Given the high compactness of the antenna, coupling between input waveguides and adjacent cavities are possibly taking place. Nevertheless, stable radiation patterns in frequency are seen, with their beam clearly pointing in broadside direction. The antenna was also manufactured (Fig. 10) and measurements were carried out, being summarized in Figs. 11 and 12.

S-parameters are shown in Fig. 11. A good matching for both operation bands of the antenna is observed. The radiation patterns (Fig. 12) show good agreement with the simulated results. Also, measured gain and antenna efficiency for different frequencies in both bands are shown in Tables I and II. A peak gain of 19 dBi in the Ka-band and 17 dBi in the K-band is obtained with a cross-polar discrimination higher than 30 dB, and average measured antenna efficiency of 80%.

IV. Conclusions

A 4×4 single-layer dual-band antenna array using Gap Waveguide technology is presented. The radiating elements consist of I-shaped slots excited by dual operation coaxial cavities, fed by a unique broadband corporate-feed network. This proof of concept proposes for the first time a full-metal single-layer dual-band GW antenna with two non-adjacent working bands. Experimental results demonstrate that the proposed array architecture is scalable and provides an appealing dual-band performance along with good impedance bandwidth and high efficiency. Some key aspects such as circular polarization performance and radiation patterns complying with regulation masks are open horizons to explore with this type of antenna.

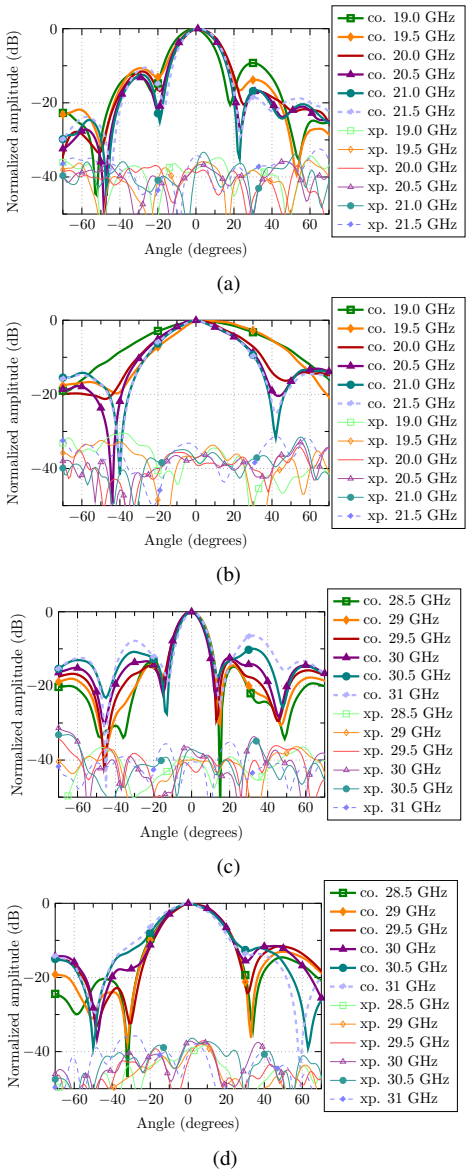

Fig. 12: Normalized copolar and crosspolar measured radiation patterns for several frequencies: K-band port (a) E-plane and (b) H-plane; Ka-band port (c) E-plane and (d) H-plane.

V. Acknowledgements

This work has been funded by the Spanish Ministry of Science and Innovation under project PID2019-107688RB-

C22.

REFERENCES

[1] Q. Zhuang and C. Zheng, "Research on inmarsat based on ka band and applications," in *2017 4th International Conference on Information, Cybernetics and Computational Social Systems (ICCSS)*. IEEE, 2017, pp. 127–129.

[2] Y. R. Ding and Y. J. Cheng, "Ku/ka dual-band dual-polarized shared-aperture beam-scanning antenna array with high isolation," *IEEE Transactions on Antennas and Propagation*, vol. 67, no. 4, pp. 2413–2422, 2019.

[3] I. Russo, C. Canestri, A. Manna, G. Mazzi, and A. Tafuto, "Dual-band antenna array with superdirective elements for short-distance ballistic tracking," *IEEE Transactions on Antennas and Propagation*, vol. 67, no. 1, pp. 232–241, 2019.

[4] J.-D. Zhang, W. Wu, and D.-G. Fang, "Dual-band and dual-circularly polarized shared-aperture array antennas with single-layer substrate," *IEEE Transactions on Antennas and Propagation*, vol. 64, no. 1, pp. 109–116, 2016.

[5] J. F. Zhang, Y. J. Cheng, Y. R. Ding, and C. X. Bai, "A dual-band shared-aperture antenna with large frequency ratio, high aperture reuse efficiency and high channel isolation," *IEEE Transactions on Antennas and Propagation*, 2018.

[6] M. Ferrando-Rocher, J. I. Herranz-Herruzo, A. Valero-Nogueira, B. Bernardo-Clemente, A. Zaman, and J. Yang, "8×8 ka-band dual-polarized array antenna based on gap waveguide technology," *Accepted for publication: IEEE Transactions on Antennas and Propagation*, vol. 67, no. 7, pp. 1–10, 2019.

[7] S. Mener, R. Gillard, and L. Roy, "A dual-band dual-circular-polarization antenna for ka-band satellite communications," *IEEE antennas and wireless propagation letters*, vol. 16, pp. 274–277, 2016.

[8] K. T. Pham, R. Sauleau, E. Fourn, F. Diaby, A. Clemente, and L. Dussopt, "Dual-band transmitarrays with dual-linear polarization at ka-band," *IEEE Transactions on Antennas and Propagation*, vol. 65, no. 12, pp. 7009–7018, 2017.

[9] H. Hasani, J. S. Silva, S. Capdevila, M. García-Vigueras, and J. R. Mosig, "Dual-band circularly polarized transmitarray antenna for satellite communications at (20, 30) ghz," *IEEE Transactions on Antennas and Propagation*, vol. 67, no. 8, pp. 5325–5333, 2019.

[10] M. Ferrando-Rocher, J. I. Herranz-Herruzo, A. Valero-Nogueira, and B. Bernardo-Clemente, "Full-metal k-ka dual-band shared-aperture array antenna fed by combined ridge-groove gap waveguide," *IEEE Antennas and Wireless Propagation Letters*, vol. 18, no. 7, pp. 1463–1467, 2019.

[11] M. Ferrando-Rocher, A. Valero-Nogueira, J. I. Herranz-Herruzo, A. Berenguer, and B. Bernardo-Clemente, "Groove gap waveguides: A contactless solution for multilayer slotted-waveguide array antenna assembly," in *2016 10th European Conference on Antennas and Propagation (EuCAP)*. IEEE, 2016, pp. 1–4.

[12] A. Vosoogh, M. S. Sorkherizi, A. U. Zaman, J. Yang, and A. A. Kishk, "An integrated ka-band diplexer-antenna array module based on gap waveguide technology with simple mechanical assembly and no electrical contact requirements," *IEEE Transactions on Microwave Theory and Techniques*, vol. 66, no. 2, pp. 962–972, 2017.

[13] A. Vosoogh, M. S. Sorkherizi, V. Vassilev, A. U. Zaman, Z. S. He, J. Yang, A. A. Kishk, and H. Zirath, "Compact integrated full-duplex gap waveguide-based radio front end for multi-gbit/s point-to-point backhaul links at e-band," *IEEE Transactions on Microwave Theory and Techniques*, vol. 67, no. 9, pp. 3783–3797, 2019.

[14] A. J. Sáez, A. Valero-Nogueira, J. I. Herranz, and B. Bernardo, "Single-layer cavity-backed slot array fed by groove gap waveguide," *IEEE Antennas and Wireless Propagation Letters*, vol. 15, pp. 1402–1405, 2015.

[15] M. Ferrando-Rocher, A. Valero-Nogueira, J. I. Herranz-Herruzo, and J. Teniente, "60 ghz single-layer slot-array antenna fed by groove gap waveguide," *IEEE Antennas and Wireless Propagation Letters*, vol. 18, no. 5, pp. 846–850, 2019.

[16] M. Ferrando-Rocher, A. Valero-Nogueira, and J. I. Herranz-Herruzo, "New feeding network topologies for high-gain single-layer slot array antennas using gap waveguide concept," in *Antennas and Propagation (EUCAP), 2017 11th European Conference on*. IEEE, 2017, pp. 1654–1657.

[17] C. Vicente, M. Mattes, D. Wolk, H. Hartnagel, J. Mosig, and D. Raboso, "Fest3d-a simulation tool for multipactor prediction," in *Proceedings on the 5th International Workshop on MULCOPIM*, 2005.